

## NUCLEAR DENSITY FUNCTIONAL THEORY

*M. Stoitsov*

Department of Physics and Astronomy, University of Tennessee Knoxville, USA

Oak Ridge National Laboratory, Oak Ridge, USA

Institute of Nuclear Research and Nuclear Energy, Bulgarian Academy of Sciences,

Sofia, Bulgaria

An understanding of atomic nuclei is crucial for a complete nuclear theory, for the nuclear astrophysics, for performing new experimental tasks, and for various other applications. Within a density functional theory, the total binding energy of the nucleus is given by a functional of the nuclear density matrices and their derivatives. The variation of the energy density functional with respect to particle and pairing densities leads to the Hartree–Fock–Bogoliubov equations. The «Universal Nuclear Energy Density Functional» (UNEDF) SciDAC project to develop and optimize the energy density functional for atomic nuclei using state-of-the-art computational infrastructure is briefly described. The ultimate goal is to replace current phenomenological models of the nucleus with a well-founded microscopic theory with minimal uncertainties, capable of describing nuclear data and extrapolating to unknown regions.

PACS: 21.60.-n

### INTRODUCTION

Density Functional Theory (DFT) has its roots in the Hohenberg–Khon theorem showing the total energy of a many-fermion system as a universal energy density functional of local density distribution  $\rho(\mathbf{r})$  — a simple quantity which depends on a spatial coordinate only, has a clear physical meaning, and can be measured experimentally.

In the nuclear case, the energy density functional depends on densities and currents (and their derivatives) representing distributions of nucleonic matter, spins, momentum, and kinetic energy. Since superconductivity plays a central role, the nuclear energy density functional is augmented by the pairing densities as well. As a result, its variation with respect to particle and pairing density matrices leads to a highly nonlinear system of Hartree–Fock–Bogoliubov (HFB) equations which has to be solved in a self-consistent manner.

Historically, the first nuclear energy density functionals appeared in the context of zero-range, density-dependent interactions such as the Skyrme force [1]. The strategy used in all modern nuclear DFT applications, however, does not assume the realistic energy density functional to be related to any given effective Hamiltonian; i.e., an effective interaction could be secondary to the functional [2].

In this way, the DFT mass calculations have achieved a quite remarkable rms deviation of the order of  $\sim 600$  keV with respect to the existing mass measurements [3].

Over the past few years, however, it has become clear that commonly used functionals suffer from various deficiencies that make it impossible to obtain a consistent and highly quantitative description of nuclear properties. For example, existing nuclear functionals remain rather poorly constrained [2,4,5] with limited predictive power when extrapolating nuclear masses away from the regions where experimental data are available, significant uncertainties regarding shell structure, and especially the energies of the single-particle states [5].

Since nuclear DFT remains the only tractable microscopic theory that can be applied across the entire table of nuclides, a lot of efforts has recently been devoted to its development.

In this short overview, some aspects of the «Universal Nuclear Energy Density Functional» SciDAC project to develop and optimize the energy density functional for atomic nuclei are briefly described.

## 1. UNEDF SciDAC COLLABORATION

The «Universal Nuclear Energy Density Functional» (UNEDF) SciDAC-2 collaboration [6] carries out a comprehensive study of all nuclei based on the most reliable theoretical approaches, the most advanced algorithms, and extensive computational resources, with a view of scaling to the petaflop platforms and beyond. We seek to replace current phenomenological models of nuclear structure and reactions with a well-founded microscopic theory that delivers maximum predictive power with well-quantified uncertainties.

One of the research tasks under UNEDF is aiming at development of the optimized nuclear energy density functional and the related computational infrastructure to solve self-consistent, nonlinear equations of the nuclear energy Density Functional Theory (DFT). The goal is to combine the best knowledge of the nuclear Hamiltonian with newly developed many-body techniques to construct a novel class of energy functionals. These functionals, validated by using the relevant data, will then be applied to predict nuclear properties and describe nuclear reactions.

From the point of view of DFT practitioners, the challenges by the UNEDF roadmap are, therefore, threefold:

- (i) What mathematical form should the energy functional take?
- (ii) Given the mathematical form, how can one optimize the functional parameters to a set of experimental data?
- (iii) How can one compute the properties of *all* atomic nuclei within a reasonable timescale?

The essence of these key roadmap challenges are further briefly addressed.

## 2. NUCLEAR ENERGY DENSITY FUNCTIONAL

Within the UNEDF project, the following general representation of the nuclear energy density functional is under consideration:

$$E = \int \mathcal{H}(\mathbf{r}) d^3\mathbf{r} = \frac{\hbar^2}{2m} \int \tau_0(\mathbf{r}) d^3\mathbf{r} + \sum_{tt'} \int \mathcal{H}_{tt'}(\mathbf{r}) d^3\mathbf{r}, \quad (1)$$

where

$$\mathcal{H}_{tt'}(\mathbf{r}) = U^{\rho_t \rho_{t'}} \rho_t \rho_{t'} + U^{\rho_t \tau_{t'}} \rho_t \tau_{t'} + U^{\rho_t \nabla J_{t'}} \rho_t \nabla \cdot \mathbf{J}_{t'} + U^{J_t J_{t'}} \mathbf{J}_t \cdot \mathbf{J}_{t'}. \quad (2)$$

The isospin index  $t = \{0, 1\}$  labels isoscalar ( $t = 0$ ) and isovector ( $t = 1$ ) densities  $\rho_t$ ,  $\tau_t$ , and  $\mathbf{J}_t$ , respectively. The isoscalar local density, for example, is the sum  $\rho_0 = \rho_n + \rho_p$  of neutron  $\rho_n$  and proton  $\rho_p$  densities, while the isovector local density is the difference  $\rho_1 = \rho_n - \rho_p$ . The same is also true for  $\tau_t$  and  $\mathbf{J}_t$ .

The diagonal energy densities  $\mathcal{H}_{tt}(\mathbf{r})$  entering Eq. (1) may appear when considering a bilinear product  $\rho V \rho$  with a two-body ( $NN$ ) interaction  $V$ . When  $V$  includes three-body ( $NNN$ ) forces, the «crossing» terms  $\mathcal{H}_{tt' \neq t}(\mathbf{r})$  may appear in Eq. (2) in such a way that the functional (1) is isospin-invariant.

The expression (2) includes six densities  $\rho_t$ ,  $\tau_t$ ,  $\mathbf{J}_t$  grouped in twenty terms multiplied by the amplitudes

$$U^m = U^m(\rho_t, \tau_t, \mathbf{J}_t, \dots), \quad (3)$$

where the superscript  $m$  stands for all twenty combinations

$$\{\rho_t \rho_{t'}, \rho_t \tau_{t'}, \rho_t \Delta \rho_{t'}, \rho_t \nabla \cdot \mathbf{J}_{t'}, \mathbf{J}_t \cdot \mathbf{J}_{t'}\}. \quad (4)$$

The assumption the amplitudes (3) could be functions of  $\rho_t$ ,  $\tau_t$ ,  $\mathbf{J}_t$  and their derivatives makes the functional representation (1) quite general.

The standard Skyrme functional follows from Eq. (1) at  $\mathcal{H}_{tt' \neq t} = 0$  and assuming the amplitudes  $U^m$  are all constants  $C^m$  with the only exception for the density-dependent amplitudes

$$C^{\rho_t \rho_t} = C_0^{\rho_t \rho_t} + C_D^{\rho_t \rho_t} \rho_0^\gamma, \quad (5)$$

which include a fractional power  $\gamma$ . Altogether, the standard Skyrme functional contains 13 parameters

$$\{C_0^{\rho_t \rho_t}, C_D^{\rho_t \rho_t}, C^{\rho_t \Delta \rho_t}, C^{\rho_t \tau_t}, C^{J_t^2}, C^{\rho_t \nabla J_t}, \gamma\}, \quad (6)$$

which are uniquely related to the well-known ( $t, x$ ) parameters [1].

A straightforward empirical generalization of the standard Skyrme functional is suggested in [7] by replacing all coupling amplitudes  $U^m$ , Eq. (3), with density-dependent functions

$$D^m = C^m + \alpha^m(1 - y_0^{\gamma^m}) + \beta^m y_1^{\eta^m}, \quad (7)$$

where  $y_0 = (\rho_0/\rho_c)$ ,  $y_1 = (\rho_1/\rho_c)^2$ , and  $\rho_c$  is the infinite nuclear matter equilibrium density. In this way the set of 13  $C$  parameters (6) is extended to a set of 68 independent parameters, i.e., 40 coupling constants  $\{C^m, \alpha^m, \beta^m\}$ , and 28 powers  $\{\gamma^m, \eta^m\}$ , thus increasing the flexibility of the functional.

Another extension of the nuclear energy density functional currently pursued comes from the Density Matrix Expansion (DME) method applied to the long-range part of chiral nucleon–nucleon interactions [8] through the leading (LO), next-to-leading (NLO), and next-to-next-to-leading (N2LO) order [9]. It retains the general structure (1) through the coupling amplitudes (3) which are of the form

$$U^m = \delta_{t,t'}(C^m + g^m(u) + \rho_0 h^m(u)) + (1 - \delta_{t,t'})\rho_1 h^m(u), \quad (8)$$

where functions  $g^m(u)$  collect all LO, NLO, and N2LO contributions from the long-range part of the  $NN$  interaction, while functions  $h^m(u)$  originate from the long-range part of the  $NNN$  interaction which appears for the first time at N2LO.

The explicit form of  $g^m(u)$  and  $h^m(u)$  offers novel density dependence of the functional as  $\log(u)$  and  $\arctan(u)$ . In the local density approximation (LDA) the Fermi momentum  $k_F$  entering the variable  $u = k_F/m_\pi$  is linked to the spatial local density distribution in the following way:

$$k_F(\mathbf{r}) = \left( \frac{3\pi^2}{2} \rho_0(\mathbf{r}) \right)^{1/3}. \quad (9)$$

It introduces, in the sense of Eq. (3), an additional  $\rho_0$ -dependence of the amplitudes  $U^m \equiv U^m(\rho_0)$ . A more complicated gradient dependence could be obtained by applying the LDA suggested by Campi and Bouyssy [10]:

$$k_F(\mathbf{r}) = \sqrt{\frac{5}{3} \frac{\tau_0(\mathbf{r}) - (1/4)\Delta\rho_0(\mathbf{r})}{\rho_0(\mathbf{r})}}, \quad (10)$$

which implies  $U^m \equiv U^m(\rho_0, \tau_0, \Delta\rho_0)$ . The mixed amplitudes additionally include the isovector density  $\rho_1$  reflecting the isospin symmetry of the functional.

Substituting the amplitudes (8) into Eq. (2), the DME functional (1) naturally splits into two terms:

$$E[\rho] = E_c[\rho] + E_\pi[\rho]. \quad (11)$$

The first term  $E_c[\rho]$  collects all contributions from the contact part of the interaction. It has exactly the same form and the same number of parameters as the

standard Skyrme functional. The second term  $E_\pi[\rho]$  originates solely from the long-range pion part of the interaction. It contains the parameters  $g_A$ ,  $f_\pi$ ,  $m_\pi$ ,  $c_1$ ,  $c_3$ ,  $c_4$ ,  $c_d$ ,  $c_e$ ,  $\Lambda_x$  of the underlying Chiral EFT interaction [8].

The underlying philosophy is that the DME can accurately capture the long-range pion physics entering  $E_\pi[\rho]$ , while one could release for optimization the parameters of the Skyrme-like functional  $E_c[\rho]$  in order to capture the missing short-range physics. Work in this area is in progress.

### 3. DFT SOLVERS

Having the form of the nuclear energy density functional, one should perform self-consistent HFB calculations in order to find the properties of a nucleus.

The coordinate-space formulation of HFB has an advantage to treat arbitrarily complex intrinsic shapes, including those seen in fission or heavy-ion fusion. A number of coordinate-space DFT solvers have been developed over the years, and their performance strongly depends on the size and symmetries of the spatial mesh employed. Of particular interest is the recently developed 2D solver HFBAX [11], based on B-splines that contain a number of enhancements resulting in a significant numerical speedup of the code. Under UNEDF, efforts are under way to develop a new-generation 3D DFT solver based on the multiresolution wavelet analysis under the MADNESS framework [12].

The configuration-space DFT solvers are based on the expansion of HFB eigenstates in a discrete basis, such as the harmonic oscillator basis. The codes that use the basis expansion technique can be very versatile. For example, the 3D DFT solver HFODD [13] is capable of treating arbitrary shapes, which is of particular importance when studying complex configurations such as high-spin states or nuclear fission. In many problems of physical interest, however, symmetry-restricted solvers are sufficient.

The computational cost of HFB iterative convergence schemes can become very expensive, especially when the size of the model space, largely determined by the imposed symmetries or the number of many-body configurations processed simultaneously, becomes huge. The HFBTHO solver [14] is a highly optimized equivalent of HFODD that is restricted to axially symmetric shapes. It is particularly adapted to large-scale nuclear mass calculations, since the vast majority of atomic nuclei are axially deformed in their ground states.

### 4. OPTIMIZATION OF THE FUNCTIONAL

In order to ensure close alignment of the necessary applied mathematics and computer science research with the necessary physics research, partnerships have been formed within the UNEDF collaboration consisting of computer scientists

and applied mathematicians linked with specific physicists. The optimization of the nuclear energy density functional is an example of such a joint effort with the mathematicians from the Argonne National Laboratory.

For values of  $p$  parameters  $\boldsymbol{\theta} \in \mathfrak{R}^p$  of a given functional, the simulators compute  $T$  observables for  $N$  nuclei:  $\{s_{t,n}(\boldsymbol{\theta})\}_{t \in T, n \in N}$ . Given an experimental data set,  $\{d_{t,n}\}_{t \in T, n \in N}$ , corresponding to different nuclear properties (such as binding energies, radii, moments), the objective is to find the parameters  $\boldsymbol{\theta}$  so that the theoretical output approximates the experimental data. To this end, we solve the nonlinear least squares problem

$$\min \left\{ f(\boldsymbol{\theta}) = \sum_{t,n} \frac{(d_{t,n} - s_{t,n}(\boldsymbol{\theta}))^2}{\sigma_{t,n}^2} : \boldsymbol{\theta} \in \mathfrak{R}^p \right\}, \quad (12)$$

where  $\sigma_{t,n} > 0$  reflects the relative accuracy of the experimental data. The optimization procedure is based on updating a quadratic model

$$q(\boldsymbol{\theta}) = f(\hat{\boldsymbol{\theta}}) + (\boldsymbol{\theta} - \hat{\boldsymbol{\theta}})^T g + \frac{1}{2}(\boldsymbol{\theta} - \hat{\boldsymbol{\theta}})H(\boldsymbol{\theta} - \hat{\boldsymbol{\theta}}), \quad (13)$$

approximating  $f(\boldsymbol{\theta})$  near the calculated solution  $\hat{\boldsymbol{\theta}}$ .

Since the Hessian  $H$  is positive semi-definite at a solution, we conduct sensitivity and correlation analysis at  $\hat{\boldsymbol{\theta}}$  as a byproduct of the optimization. Under certain statistical assumptions,  $H$  can be used to approximate the covariance

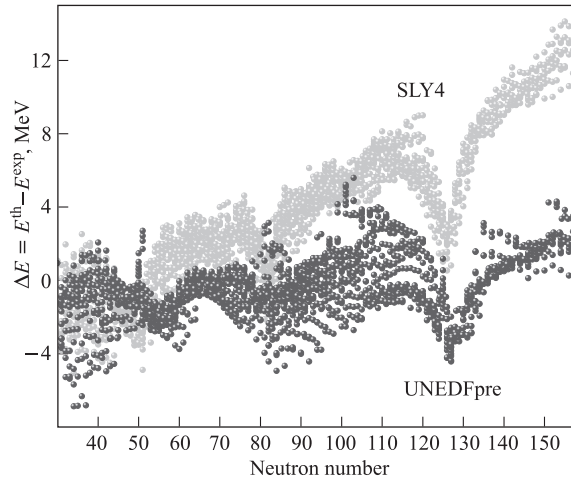


Fig. 1. Differences between experimental binding energies and theoretical results obtained with the standard Skyrme functional for two different sets of parameters: SLY4 [15] and UNEDFpre [16]

$\text{Cov}(\boldsymbol{\theta}) \approx H^{-1}$ , and hence the correlation matrix

$$R_{ij} = \frac{\text{Cov}_{ij}(\boldsymbol{\theta})}{\sqrt{\text{Cov}_{ii}(\boldsymbol{\theta})\text{Cov}_{jj}(\boldsymbol{\theta})}}. \quad (14)$$

Such an analysis is a standard approach in other domains of physics, but could not be addressed in nuclear structure until very recently due to the extremely high cost of the function evaluations. Recent progress in code development and hardware architectures, however, made it possible to undertake such a global parameter search with a consequent statistical analysis of the nuclear functional.

As an example, the difference between experimental masses and theoretical results obtained with newly optimized standard Skyrme functional [16] is illustrated in Fig. 1. To generate the functional UNEDFpre [16], the HFBTHO solver has been used as a simulator for the optimization (12)–(14) carried out for 108 observables — binding energies, rms-radii, and pairing gaps for a set of 72 spherical and deformed nuclei.

## 5. LARGE SCALE NUCLEAR MASS TABLE

Calculating the entire nuclear mass table is a challenge of its own. Around 10,000 nuclei are expected to exist between the proton and neutron limits of stability, representing about 600,000 many-body configurations for which an HFB solution needs to be found. They are either spherical (quadrupole deformation  $\beta = 0$ ), prolate ( $\beta > 0$ ), or oblate ( $\beta < 0$ ).

In order to determine the ground-state equilibrium deformation, constrained calculations are first carried out for every nucleus on a  $\beta$ -deformation grid. The resulting energy curves define the regions within which the local minima are found. The ground-state configuration is assigned to the lowest-energy minimum.

In the nuclear DFT, the ground state of an odd-mass nucleus is represented by the blocking of a one-quasi-particle excitation out of a paired HFB vacuum representing a neighboring even–even system [17]. The quantum numbers of the quasi-particle excitation that yield the lowest total energy are not known beforehand; hence, one must select several blocking candidates in a given energy window around the Fermi level.

In HFBTHO, the quasi-particle calculations are carried out for each configuration within the so-called equal-filling approximation, which preserves the time-reversal symmetry. Odd–odd nuclei are handled by a double-blocking procedure: for each blocked one-quasi-neutron state, we solve the HFB equations by considering all possible one-quasi-proton states within the energy cutoff range, and the lowest-energy final state is assigned to the ground state of the odd–odd system. The total number of different configurations to be taken into account across the mass table is of the order of one million.

In spite of the high efficiency of HFBTHO, computing the entire mass table would take almost 12 CPU years on a single processor. However, with the help of massively parallel computers such as the Cray XT5 Jaguar and Kraken, the entire calculation is accomplished in a single 14-CPU-hour run involving 9,000 processors. As an illustrative example, Fig. 2 shows the result of a large-scale HFBTHO mass-table run with the UNEDFpre Skyrme functional [16] and a zero-range pairing force covering all even–even, odd–even, and odd–odd nuclei with neutron number  $2 \leq N \leq 190$  and proton number  $2 \leq Z \leq 110$ . For some recent applications of mass-table results, see [18].

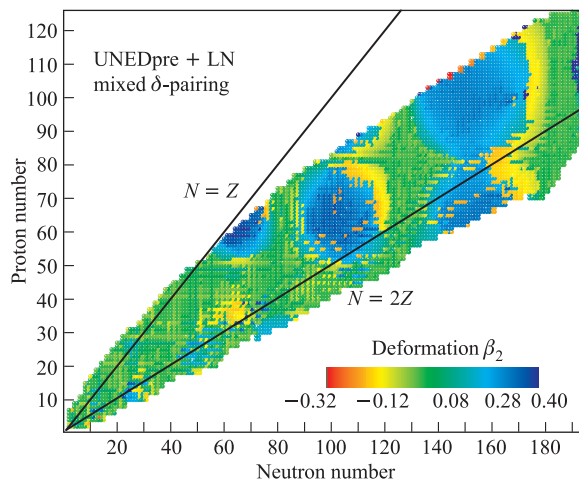


Fig. 2. Ground-state shape deformation of even–even, odd–even, and odd–odd atomic nuclei across the entire nuclear chart obtained in a single mass-table run on the Cray XT5 Jaguar supercomputer. The calculations were carried out with the HFBTHO solver using the energy density functional UNEDFpre [16] augmented by density-dependent zero-range pairing force

The complexity of the large-scale nuclear mass table problem cannot be resolved by a trivial increase in the number of processors used. To find converged DFT results for the multitude of nuclear configurations is a challenging task that requires the development of efficient DFT solvers, optimized for leadership-class architectures.

One of the crucial enhancements, proposed and analyzed in detail in [19], is the use of the modified Broyden mixing for the numerical solution of nonlinear equations in many variables to nuclear self-consistent calculations. This method provides impressive performance improvements against the conventional linear-mixing procedure. For example, using linear mixing, one is left with almost

30% unconverged cases assuming the standard accuracy requirements. With the Broyden method, all nuclei shown in Fig. 2 are resolved.

## 6. VISUALIZATION TOOLS

One of the bottlenecks in large-scale calculations is the massive amount of data produced in mass-table runs. Specialized tools must be developed to analyze and exploit this rich theoretical output. To this end, a web server has been dedicated to collecting, sorting, and visualizing the data produced by UNEDF mass-table runs. It can be freely accessed at <http://massexplorer.org>. The web site contains links to the raw data files, and more useful data will become available as the UNEDF project progresses.

From the <http://massexplorer.org> web site, one can download a powerful visualization tool written in Java, Mass Table Explorer (MTeX), which offers visualization, manipulation, and access to the numerical values and graphical representations of the data.

Its online version, WebMTeX, allows one to perform online DFT «calculations» right from the browser by utilizing all the pre-calculated mass-table data sets available. The output is displayed in the browser as image files or data grids that can be further copied and manipulated.

## CONCLUSIONS

We have presented a short overview of the current status of one of the research tasks under the UNEDF SciDAC project aiming to develop key computational codes and algorithms for reaching the goal of solving the nuclear quantum many-body problem, thus paving the road to the comprehensive model of the nucleus.

Finding the nuclear energy density functional for atomic nuclei capable of describing stable and short-lived nuclei and their reactions requires the unique combination of innovative theoretical tools that can link microscopic interactions to energy functionals, significant code development with special emphasis on massively parallel algorithms, and state-of-the-art optimization techniques that can efficiently cope with the high computational cost of function evaluations.

**Acknowledgements.** M. S. would like to thank Victor Voronov, Rostislav Jolos, and Elena Kolganova for their kind and warm hospitality.

The DFT/Optimization UNEDF team includes M. Kortelainen, T. Lesinski, J. McDonnell, W. Nazarewicz, N. Nikolov, J. C. Pei, N. Schunck, and M. Stoitsov from ORNL/UT; G. I. Fann, H. A. Nam, and W. A. Shelton from ORNL; J. Moré, J. Sarich, and S. Wild from ANL; D. Furnstahl (OSU); S. K. Bogner and Biruk

Gebremariam (NSCL/MSU); J. Dobaczewski (Warsaw/Jyväskylä), and T. Duguet (Saclay).

The UNEDF SciDAC collaboration is supported by the Office of Science, U. S. Department of Energy, grant No. DOE-FC02-09ER41583. This work was also supported by DOE Contract Nos. DE-FG02-96ER40963 (University of Tennessee), DE-FG05-87ER40361 (Joint Institute for Heavy Ion Research), and DE-FG03-03NA00083 (Stewardship Science Academic Alliances).

## REFERENCES

1. *Negele J. W.* // Phys. Rev. C. 1970. V. 1. P. 1260;  
*Vautherin D., Brink D. M.* // Phys. Rev. C. 1972. V. 5. P. 626;  
*Negele J. W., Vautherin D.* // Ibid. P. 1472.
2. *Stoitsov M. et al.* // Intern. J. Mass Spectrometry. 2006. V. 251. P. 243.
3. *Goriely S., Chamel N., Pearson J. M.* // Phys. Rev. Lett. 2009. V. 102. P. 152503.
4. *Bertsch G. F., Sabbey B., Uusnäkki M.* // Phys. Rev. C. 2005. V. 71. P. 054311.
5. *Kortelainen M. et al.* // Phys. Rev. C. 2008. V. 77. P. 064307.
6. *Bertsch G. F., Dean D. J., Nazarewicz W.* SciDAC Review. 2007. P. 42;  
<http://www.unedf.org>.
7. *Kortelainen M. et al.* To be published.
8. *Epelbaum E., Glöckle W., Meißner U.-G.* // Nucl. Phys. A. 2005. V. 747. P. 362;  
*Epelbaum E. et al.* // Phys. Rev. C. 2002. V. 66. P. 064001.
9. *Gebremariam B., Duguet T., Bogner S. K.* nucl-th/0910.4979v3.
10. *Campi X., Bouyssy A.* // Phys. Lett. B. 1978. V. 73. P. 263.
11. *Pei J. C. et al.* // Phys. Rev. C. 2008. V. 78. P. 064306.
12. *Yanai T. et al.* // J. Chem. Phys. 2004. V. 121. P. 2866.
13. *Dobaczewski J. et al.* // Comp. Phys. Commun. 2009. V. 180. P. 2361.
14. *Stoitsov M. V. et al.* // Comp. Phys. Commun. 2005. V. 167. P. 43.
15. *Chabanat E. et al.* // Nucl. Phys. A. 1998. V. 635. P. 231.
16. *Kortelainen M. et al.* To be published.
17. *Bertsch G. et al.* // Phys. Rev. A. 2009. V. 79. P. 043602.
18. *Bertsch G. F. et al.* // Phys. Rev. C. 2009. V. 79. P. 034306;  
*Stoitsov M., Nazarewicz W., Schunck N.* // Intern. J. Mod. Phys. E. 2009. V. 18.
19. *Baran A. et al.* // Phys. Rev. C. 2008. V. 78. P. 014318.